



Active simultaneous uplift and margin-normal extension in a forearc high, Crete, Greece



S.F. Gallen^{a,*}, K.W. Wegmann^a, D.R. Bohnenstiehl^a, F.J. Pazzaglia^b, M.T. Brandon^c, C. Fassoulas^d

^a Department of Marine, Earth and Atmospheric Sciences, North Carolina State University, Raleigh, NC, USA

^b Department of Earth and Environmental Sciences, Lehigh University, Bethlehem, PA, USA

^c Department of Geology and Geophysics, Yale University, New Haven, CT, USA

^d Natural History Museum of Crete, University of Crete, Heraklion, Greece

ARTICLE INFO

Article history:

Received 17 March 2014

Received in revised form 18 April 2014

Accepted 22 April 2014

Available online xxxx

Editor: P. Shearer

Keywords:

tectonic geomorphology

marine terrace

normal fault

uplift

underplating

ABSTRACT

The island of Crete occupies a forearc high in the central Hellenic subduction zone and is characterized by sustained exhumation, surface uplift and extension. The processes governing orogenesis and topographic development here remain poorly understood. Dramatic topographic relief (2–6 km) astride the southern coastline of Crete is associated with large margin-parallel faults responsible for deep bathymetric depressions known as the Hellenic troughs. These structures have been interpreted as both active and inactive with either contractional, strike-slip, or extensional movement histories. Distinguishing between these different structural styles and kinematic histories here allows us to explore more general models for improving our global understanding of the tectonic and geodynamic processes of syn-convergent extension. We present new observations from the south-central coastline of Crete that clarifies the role of these faults in the late Cenozoic evolution of the central Hellenic margin and the processes controlling Quaternary surface uplift. Pleistocene marine terraces are used in conjunction with optically stimulated luminescence dating and correlation to the Quaternary eustatic curve to document coastal uplift and identify active faults. Two south-dipping normal faults are observed, which extend offshore, offset these marine terrace deposits and indicate active N–S (margin-normal) extension. Further, marine terraces preserved in the footwall and hanging wall of both faults demonstrate that regional net uplift of Crete is occurring despite active extension. Field mapping and geometric reconstructions of an active onshore normal fault reveal that the subaqueous range-front fault of south-central Crete is synthetic to the south-dipping normal faults on shore. These findings are inconsistent with models of active horizontal shortening in the upper crust of the Hellenic forearc. Rather, they are consistent with topographic growth of the forearc in a viscous orogenic wedge, where crustal thickening and uplift are a result of basal underplating of material that is accompanied by extension in the upper portions of the wedge. Within this framework a new conceptual model is presented for the late Cenozoic vertical tectonics of the Hellenic forearc.

© 2014 Elsevier B.V. All rights reserved.

1. Introduction

The Hellenic Subduction zone is the largest, fastest and most seismically active subduction zone in the Mediterranean, where the African slab subducts beneath Crete at a rate of $\sim 36 \text{ mm yr}^{-1}$ (Fig. 1; McClusky et al., 2000; Reilinger et al., 2006). Cenozoic

subduction resulted in the construction of a large south-facing orogenic wedge spanning from the northern coastline of Crete to the surface expression of the subduction trench (e.g., Willett et al., 1993; Rahl et al., 2005; Wegmann, 2008; Jolivet and Brun, 2010). The leading edge of the subduction zone is obscured beneath a thick package of sediments and is often misidentified as the more inboard bathymetric depressions known as the Hellenic troughs, but it is actually located outboard of the Mediterranean Ridge accretionary complex, $\sim 150 \text{ km}$ south of Crete (Fig. 1; Ryan et al., 1982; Kastens, 1991; Chamot-Rooke et al., 2005). The topographic development of prominent forearc highs (e.g. Crete, Rhodes) is controlled by ongoing convergence and characterized by rapid, broad, sustained uplift with widespread upper-crustal

* Corresponding author at: Department of Earth and Environmental Sciences, University of Michigan, Ann Arbor, MI, USA. Tel.: +1 734 7642466; fax: +1 734 7634690.

E-mail addresses: sfgallen@umich.edu (S.F. Gallen), karl_wegmann@ncsu.edu (K.W. Wegmann), drbohnens@ncsu.edu (D.R. Bohnenstiehl), fjp3@lehigh.edu (F.J. Pazzaglia), mark.brandon@yale.edu (M.T. Brandon), fassoulas@nhmc.uoc.gr (C. Fassoulas).

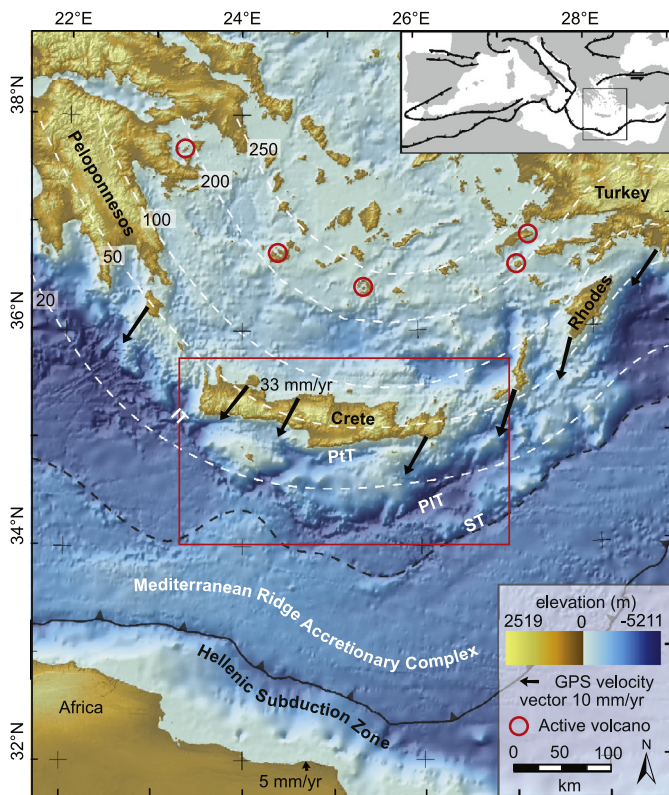


Fig. 1. Tectonic setting of the eastern Mediterranean in the vicinity of Crete, Greece. Inset: map of the major active and inactive convergent boundaries in the Mediterranean region and the North Anatolian Fault. The box highlights the area of the larger map. The Hellenic troughs, including the Ionian (IT), Ptolemy (PrT), Pliny (PIT), and Strabos (ST) are labeled. The location of the Hellenic Subduction zone in the south and back thrust (black dashed line) to the north that define the boundaries of the Mediterranean Ridge Accretionary complex is from Kreemer and Chamot-Rooke (2004). The GPS velocity vectors (black arrows) are resolvable into a total convergence rate of ~ 36 mm/yr (Reilinger et al., 2006). Depth (km) to the subducting plate (dashed white lines) is from Benioff-zone seismicity (Papazachos et al., 2000), micro-seismicity (Meier et al., 2004; Becker et al., 2006), and an upper mantle seismic velocity model (Gudmundsson and Sambridge, 1998). The red box shows the location of Fig. 2. (For interpretation of the references to color in this figure legend, the reader is referred to the web version of this article.)

extension (Angelier et al., 1982; Knapmeyer and Harjes, 2000; Rahl et al., 2005). Despite more than 40-years of geologic and geophysical investigations in the eastern Mediterranean, the tectonic and geodynamic processes governing uplift and extension of the Hellenic forearc remain contentious.

Essential to this debate are the kinematics and activity of a series of large arc-parallel faults and associated escarpments embedded in the forearc that are related to the construction of the Hellenic troughs and bound Crete's southern coastline (Figs. 1, 2). Two sets of faults dominate the central Hellenic margin; N–S striking extensional faults (Taymaz et al., 1990; Nyst and Thatcher, 2004; Bohnhoff et al., 2005; Shaw and Jackson, 2010) and much larger approximately E–W striking structures that are oriented sub-parallel to the high topographic and bathymetric relief (Figs. 1, 2; Angelier et al., 1982; Peterek and Schwarze, 2004). The N–S striking structures are unambiguously active normal faults as indicated by Holocene fault scarps and earthquake focal mechanisms (Bohnhoff et al., 2005; Caputo et al., 2006; Shaw and Jackson, 2010). However, a diversity of opinions exists as to the activity and kinematics of the larger E–W striking faults, with interpretations ranging from active to inactive, and including contractional, strike-slip and extensional; depending in part upon the dataset used to interpret displacement history (e.g. Angelier et al., 1982; Meulenkamp et al., 1988, 1994; Taymaz et al., 1990; Bohnhoff et

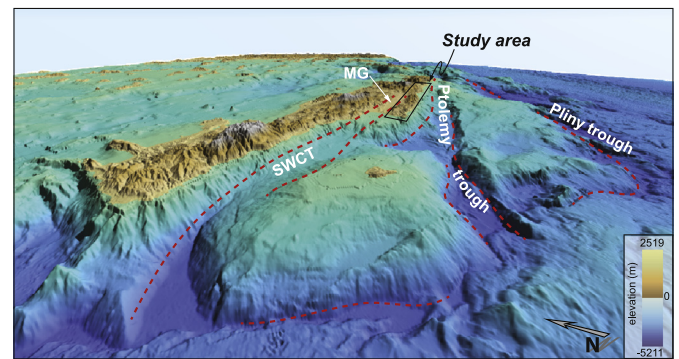


Fig. 2. Perspective view of digital topography (ASTER-topography, GEBCO-bathymetry) of the central Hellenic forearc highlighting the E–W striking structures that are the focus of this investigation, including the Southwest Cretan trough (SWCT) and Messara Graben (MG). Note the scale and dramatic topographic relief (2–6 km) associated with these faults. The N–S striking extensional faults are difficult to discern at the scale of the map and are thus not highlighted. The rectangle outlines the study area shown in Fig. 3.

al., 2001; Ring et al., 2001, 2003; ten Veen and Kleinspehn, 2003; Kreemer and Chamot-Rooke, 2004; Peterek and Schwarze, 2004; Rahl et al., 2005; Meier et al., 2007; Becker et al., 2010; Shaw and Jackson, 2010; Özbakır et al., 2013). The correctness of one model versus another has direct implications for the processes driving orogenesis above the Hellenic subduction zone as well as the potential seismic hazard posed by these faults.

Le Pichon and Angelier (1981) argued that Crete is a rigid backstop, and that uplift of the island was due to sediment underplating beneath this backstop. However, the presence of young, deeply exhumed high-pressure metamorphic rocks and active normal faults on the island are observations contrary to the hypothesis of a rigid backstop (e.g. Angelier et al., 1982; Fassoulas et al., 1994; Bohnhoff et al., 2001). Exhumation of the high-pressure metamorphic units is interpreted to have occurred by N–S (margin-normal) extension on E–W striking faults (Angelier et al., 1982; Fassoulas et al., 1994; Jolivet et al., 1996; Ring and Layer, 2003). Meulenkamp et al. (1988, 1994), Taymaz et al. (1990), and Shaw and Jackson (2010) posited that margin-normal extension has ceased and margin-normal shortening is now active on the Hellenic trough faults, resulting in the crustal thickening and uplift of Crete. Some researchers hypothesize that the E–W striking faults now accommodate sinistral strike-slip motion (ten Veen and Kleinspehn, 2003), while others argue that these structures continue to accommodate margin-normal extension (Angelier et al., 1982; Ring et al., 2001, 2003; Peterek and Schwarze, 2004). In these latter cases, upper crustal shortening is unlikely, requiring ongoing underplating to thicken the crust and raise Crete above the geoid as shown by Knapmeyer and Harjes (2000) and argued by Ring and Layer (2003).

Here we present new observations that show that margin-normal extension in the Hellenic forearc continues to the present and acts in concert with rapid, sustained uplift. Our study focuses on the tectonic geomorphology of the southern coastline of central Crete adjacent to the Ptolemy trough, one of the Hellenic troughs, where multiple sets of E–W striking faults extend offshore. South-central Crete is opportunistically situated to determine the activity and kinematics of these E–W striking faults and elucidate the processes that dictate ongoing orogenesis above the Hellenic subduction zone (Fig. 2). Pleistocene marine terraces are used in conjunction with optically simulated luminescence (OSL) and correlations to the Quaternary eustatic curve to document the rates and patterns of coastal uplift and identify active faults. Structural mapping, fault scaling properties and fault aspect ratios are used to determine the size of onshore faults and for testing hypothesized geometries and kinematics of the Ptolemy trough fault

(Figs. 1, 2). Our results demonstrate that E–W striking faults in southern Crete are actively accommodating margin-normal extension, which in turn is outpaced by regional uplift. We discuss our results in the context of the debate surrounding the processes driving ongoing orogenesis in the Hellenic forearc and conclude by presenting a new conceptual model for the late Cenozoic topographic and geodynamic evolution of the Hellenic subduction zone.

2. Background

2.1. Tectonic and geodynamic setting

A well-defined Benioff seismic zone illuminates the Hellenic subduction interface as it dips northward at 10° to 15°, reaching depths of 35 to 45 km beneath Crete and many hundreds of kilometers beneath the central Aegean (e.g. Papazachos et al., 1996, 2000; Knapmeyer, 1999; van Hinsbergen et al., 2005). Seismic tomography has imaged the subducted slab to depths > 600 km (Spakman et al., 1988; Wortel and Spakman, 2000), while Mesozoic to Cenozoic arc volcanism (Pe-Piper and Piper, 2002) from the Aegean and eastern Mediterranean show that the Hellenic subduction zone has continued to consume the African plate since at least 100 Ma (Faccenna et al., 2003; van Hinsbergen et al., 2005). Directional younging of arc volcanism (Pe-Piper and Piper, 2002, 2006, 2007) and high-pressure metamorphic rocks (Seidel et al., 1982; Wijbrans and McDougall, 1986, 1988; Theye et al., 1992; Jolivet et al., 1996; Liati and Gebauer, 1999; Tomaschek et al., 2003) in the Aegean indicates that the trench has migrated southward relative to Eurasia since at least 15 Ma, and likely as early as the Eocene (Faccenna et al., 2003; Brun and Sokoutis, 2007, 2010; Georgiev et al., 2010; Jolivet and Brun, 2010; Ring et al., 2010). The Hellenic subduction complex can thus be viewed as a southward migrating “orogenic wave” akin to other well-studied retreating subduction systems (e.g., Royden, 1993), such as the Apennines of Italy (e.g. Picotti and Pazzaglia, 2008; Thomson et al., 2010; Bennett et al., 2012).

2.2. Geologic and tectonic summary of Crete

The crust underlying Crete is composed of compressional nappes that were emplaced from the late Cretaceous onward (Jolivet and Brun, 2010 and references therein). Latest Oligocene to early Miocene (24 to 19 Ma) ages of peak metamorphism from nappe units (Theye and Seidel, 1993) indicates that they were subducted prior to a middle Miocene (18 to 10 Ma) period of rapid exhumation (Thomson et al., 1998; Brix et al., 2002; Rahl et al., 2005; Jolivet and Brun, 2010; Marsellos et al., 2010). Southward extension of the Aegean domain initiated at approximately 23 Ma, and horizontal brittle extension has dominated near the surface since the Miocene (Angelier et al., 1982; Bohnhoff et al., 2001; Fassoulas, 2001; Ring et al., 2001; Peterek and Schwarze, 2004; Zachariasse et al., 2008; van Hinsbergen and Schmid, 2012) and continues today in the vicinity of Crete (Fassoulas et al., 1994; Bohnhoff et al., 2005; Caputo et al., 2006). On Crete, extensional faults cut the nappes and opened basins that filled with Miocene to Pliocene marine sediments that are now exposed 100's of meters above sea-level, indicating long-lived uplift of the island (Meulenkamp et al., 1994; van Hinsbergen and Meulenkamp, 2006; Zachariasse et al., 2008). Quaternary uplift is observed in Pleistocene and Holocene paleo-shoreline markers found 10's to 100's of meters above modern sea level along the coastlines of Crete (Flemming, 1978; Angelier, 1979; Pirazzoli et al., 1982; Meulenkamp et al., 1994; Kelletat, 1996; Wegmann, 2008; Strasser et al., 2011).

3. Methods

3.1. Field investigation

Field investigations focused upon the spatial and temporal arrangement of Pleistocene marine terraces and alluvial fans along the south-central coast of Crete. Marine terrace inner shoreline angle (ISA) elevations, which approximate paleo-sea level at the time of terrace formation (Lajoie, 1986; Merritts and Bull, 1989), were measured from flights of terraces at 18 sites along the south-central coastline of Crete using differential GPS (Fig. 3). ISA elevation measurement errors varied between 0.1 to 4 m, after post-processing corrections were applied (Gallen, 2013). Terraces were correlated along the coastline by GPS survey elevation, stratigraphic relationships, and the degree of soil development in overlying alluvial fans. The variation in properties, such as the accumulation of pedogenic carbonate or illuvial clays in the soil B-horizon, between soils developed on alluvial fans of different age can be used for relative dating and stratigraphic correlation (e.g., Birkeland, 1984). Faults identified in the field that offset marine terraces and alluvial fans were mapped and their surface orientations measured using standard methods.

3.2. Optically stimulated luminescence (OSL) geochronology

Fine-grained lenses of quartz-rich sediment from marine terraces and alluvial fans were collected to determine the timing of sediment burial using OSL. Standard sampling and laboratory preparation techniques were applied to each sample prior to dating. All samples were analyzed at the Labor Scientific Luminescence Dating Laboratory. The single aliquot regenerative-dose (SAR) protocol was adopted for equivalent dose (D_e) measurements on twenty-four aliquots per sample (e.g. Rhodes, 2011). The final reported D_e is the average of all aliquots and the associated standard error of the mean (68%) for each sample. The cosmic ray dose rate was estimated as a function of depth, altitude and geomagnetic latitude. Additional samples collected at each site were used to measure the concentration of U, Th, and K by neutron activation analysis in the laboratory and elemental concentrations were then converted into an annual dose rate, taking into account the water content effect.

3.3. Rates of coastal uplift and eustatic correlations

Pleistocene (10^4 to 10^5 yr) uplift rates were determined by height-age relationships for the OSL-dated marine terraces. The uplift rate, u , and its standard error, $SE(u)$, are calculated from the following:

$$u = \Delta H / T, \quad (1)$$

and

$$SE(u)^2 = u^2 \left(\left(\frac{\sigma_{\Delta H}^2}{\Delta H^2} \right) + \left(\frac{\sigma_{t_T}^2}{t_T^2} \right) \right), \quad (2)$$

where t_T is the age of the terrace with a standard error, $SE(t_T)$, and ΔH is the change in height of the terrace since the time it was beveled:

$$\Delta H = H_T - \delta H_{SL}, \quad (3)$$

where H_T is present elevation of the marine terrace ISA above modern mean sea-level and δH_{SL} is the eustatic elevation for the dated terrace time interval. $SE(\Delta H)$ is the standard error for the tectonic uplift ($SE(H_T)^2 + SE(\delta H_{SL})^2$). The terrace elevation standard error, $SE(H_T)$, is based on the analytical uncertainty associated

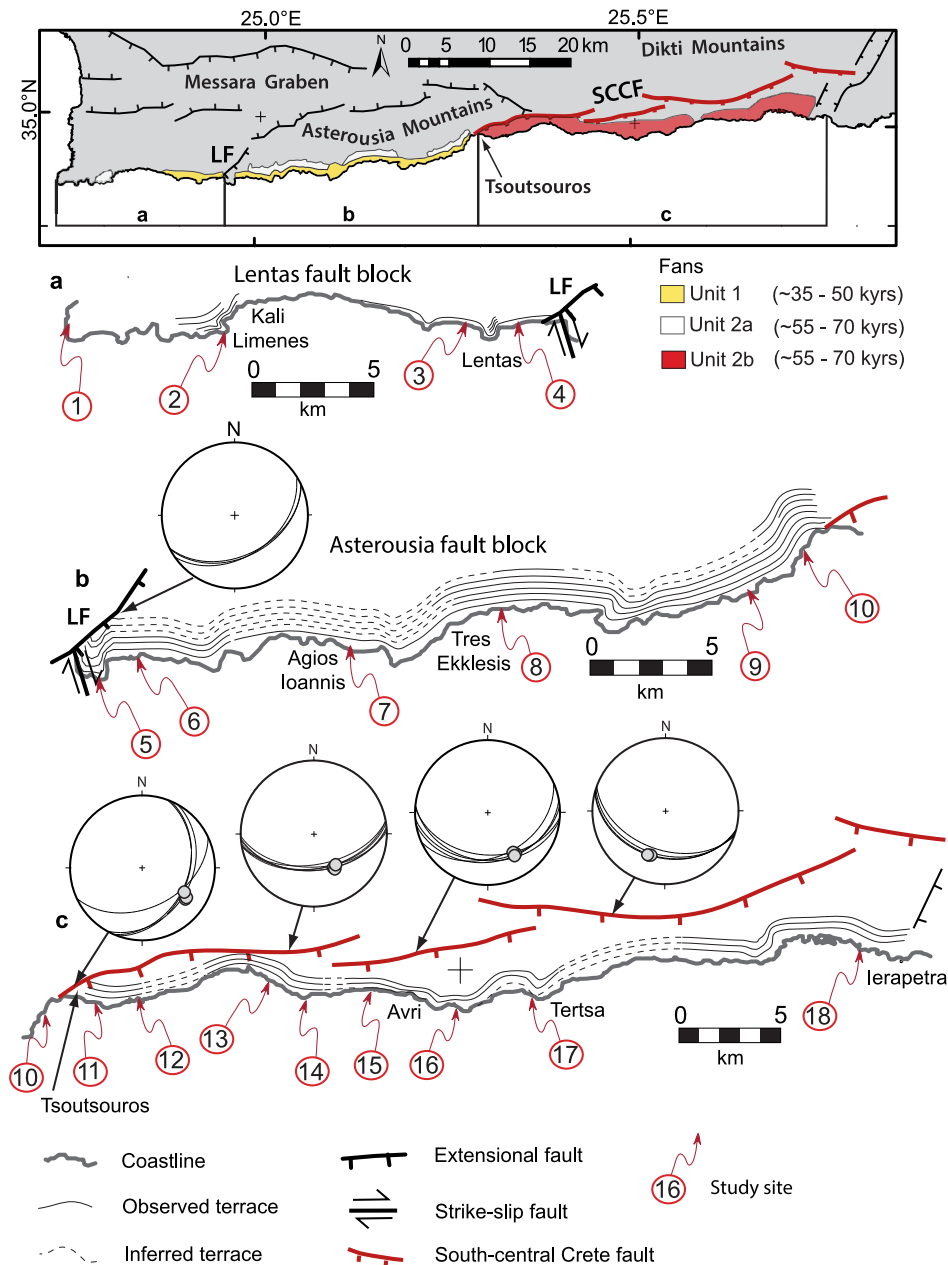


Fig. 3. Map of south-central Crete with the geographic distribution of alluvial fans and marine terraces observed in the field (fan map units not to scale). (a–c) Along-coast distribution of Pleistocene marine terraces from south-central Crete. These figures are not drafted to scale, thus the vertical separation between terraces is relative. The strike and dip of fault plane measurements and the trend and plunge of slicken-line measurements are plotted on equal area projections as great circles and points, respectively. Sites 1 to 18 are keyed to Supplementary Tables S1–S3. The location of the Lentas Fault (LF) is noted on maps a and b. The South-Central Crete fault (SCCF) is shown in red on map c. (For interpretation of the references to color in this figure legend, the reader is referred to the web version of this article.)

with the differential GPS system used to measure terrace elevations. Standard errors in sea level, $SE_{(\delta_{HSL})}$, arise from the observational data and methods used to reconstruct sea level history (e.g., Lambeck and Chappell, 2001; Waelbroeck et al., 2002).

We appeal to a general model in which Pleistocene marine terraces form during periods of relative sea-level stability, such as during glacio-eustatic highstands (Lajoie, 1986; Merritts and Bull, 1989). Geochronologic dating of at least one terrace at a particular locality allows for local calibration of the entire terrace flight to the Quaternary eustatic curve assuming that the uplift rate remains positive. We model steady or unsteady uplift based on geochronologic results and alternative correlations of marine terraces to the eustatic curve (e.g. Merritts and Bull, 1989). The age and uncertainty for a given sea level highstand is assigned to a

corresponding terrace for calculation of uplift rates using Eqs. (1) through (3).

4. Results

4.1. Faults

Two south-dipping normal faults extend offshore, offset Pleistocene marine terraces and divide the study area into three distinct fault blocks: the Lentas and Asterousia fault blocks and the hanging wall of the South-Central Crete fault (Fig. 3). The more westerly of the two faults, the Lentas fault, strikes ENE and dips 45° south-southeast (Fig. 3). No slip indicators were observed on this fault. The Lentas fault vertically offsets the lowest terrace in the sequence by 14.5 ± 1 m.

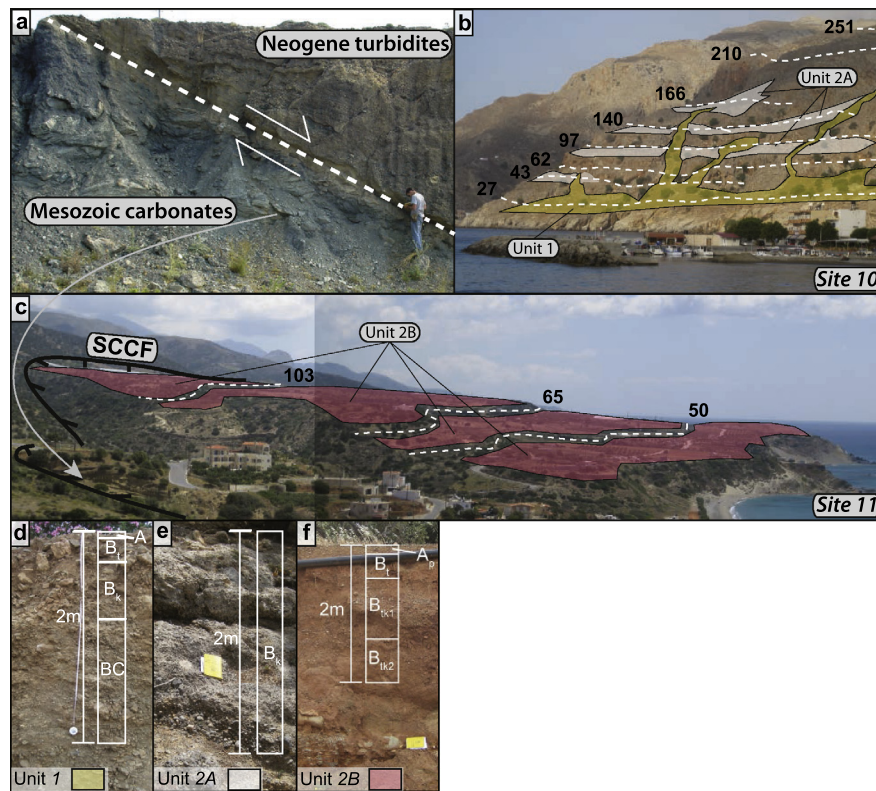


Fig. 4. (a) Photo of an exposure of the South-Central Crete fault in Tsoutsouros. The gray arrow indicates the location of the photo in (c). (b–c) Photos of alluvial fan and marine terrace stratigraphy at sites 10 and 11 (see Fig. 3 for location). The white dashed lines show the approximate inner shoreline elevation of surveyed marine terraces, while the number correspond to their elevations in meters above present-day sea level. The colored polygons show the extent and type of alluvial fans observed at each site and the colors are keyed to (d–e). Note the inset relationship between fan Unit 1 and Unit 2A in (b). (d–f) Photos of the three fan and soil-type pairs identified in the study area. (For interpretation of the references to color in this figure legend, the reader is referred to the web version of this article.)

The more easterly South-Central Crete fault extends offshore at Tsoutsouros, forms the segmented front of the Dikti Mountains, and terminates about 55 km to the east of its first onshore exposure (Fig. 3). The South-Central Crete fault has four main segments that dip 40° to 50° south and juxtaposes Mesozoic rocks in the footwall against Neogene units in the hanging wall (Figs. 3c, 4a). Exposed fault planes contain slickenlines demonstrating predominantly dip-slip motion (Fig. 3c). The South-Central Crete fault unequivocally offsets late Quaternary marine terraces west of Tsoutsouros (Figs. 3, 4; sites 10 and 11). Well-preserved fault scarps in bedrock are found along the footwalls of all fault segments, and bedrock stream channel convexities (knickpoints) are common immediately upstream from the surface fault trace, providing evidence of recent activity along the entire length of the fault (Gallen, 2013). The observation that Pleistocene marine terraces are offset and preserved in both the footwall and hanging wall of the Lentas and South-Central Crete faults highlights the fact that regional uplift outpaces hanging wall subsidence in southern Crete. Subaerially-exposed Neogene marine sediments in the hanging wall of the South-Central Crete fault indicates this condition has persisted throughout much of the late Cenozoic (Zachariasse et al., 2008).

4.2. Marine terraces and alluvial fans

Marine terraces and bio-erosional notches with ISA elevations that vary between 1 and 260 m above mean sea level (amsl) are extensive and easily defined along the south coast of central Crete (Fig. 4; Supplementary Table 1S). Some terraces are buried by >2 m-thick alluvial fan deposits, which limits estimation of the ISA elevation to a minimum value. Local geology and coastline geography play an important role in the form and preservation of the ter-

aces (Supplementary Fig. 1S). Well-defined and preserved terraces and paleo-shoreline notches are found where Mesozoic carbonates, sandstones and mudstones crop out (Fig. 4b); although their width is often of limited extent. Laterally-extensive marine terraces are often preserved in Neogene units (Fig. 4c). In contrast, terraces are almost completely absent from coastal areas underlain by Mesozoic ophiolitic sequences, due to the enhanced mass-wasting potential of these units in comparison to the other rock-types.

We distinguish three distinct mappable alluvial fan units, based on sedimentologic and stratigraphic characteristics and relative surface age determined from the degree and nature of soil development (Fig. 4d–f). Fan units 1 and 2A are present along the coast of the Lentas and Asterousia fault blocks. The sedimentology of Units 1 and 2A is indistinguishable, but differ stratigraphically and in the degree of surface soil development (Fig. 4b, d, e). Unit 1 fans are younger and are topographically inset into Unit 2A, exhibiting thin mineral A soil horizons, weakly-developed illuvial horizons (Bt), and local incipient calcic horizons (Bk; Fig. 4d). By contrast, Unit 2A fans have a diagnostic well-developed petrocalcic soil horizon (Bk) that may or may not be capped by a thin mineral A soil horizon (Fig. 4e). Unit 2B alluvial fans are only found in the hanging wall of the South-Central Crete fault (Figs. 3, 4), are generally thicker and composed of smaller, more rounded clasts than Unit 1 or 2A fans (Fig. 4f). They exhibit soils with thin, well-developed mineral A horizons and thick, red, Btk horizons. Alluvial fan treads preserved along the south-central coastline are all graded to a base level far lower than present-day sea level, indicating that the timing of fan progradation occurred during eustatic lowstands.

The marine terraces and alluvial fans in south-central Crete form a coastal stratigraphy unique to the three fault-bounded blocks (Figs. 3, 4). In the Lentas fault block, a four-terrace sequence

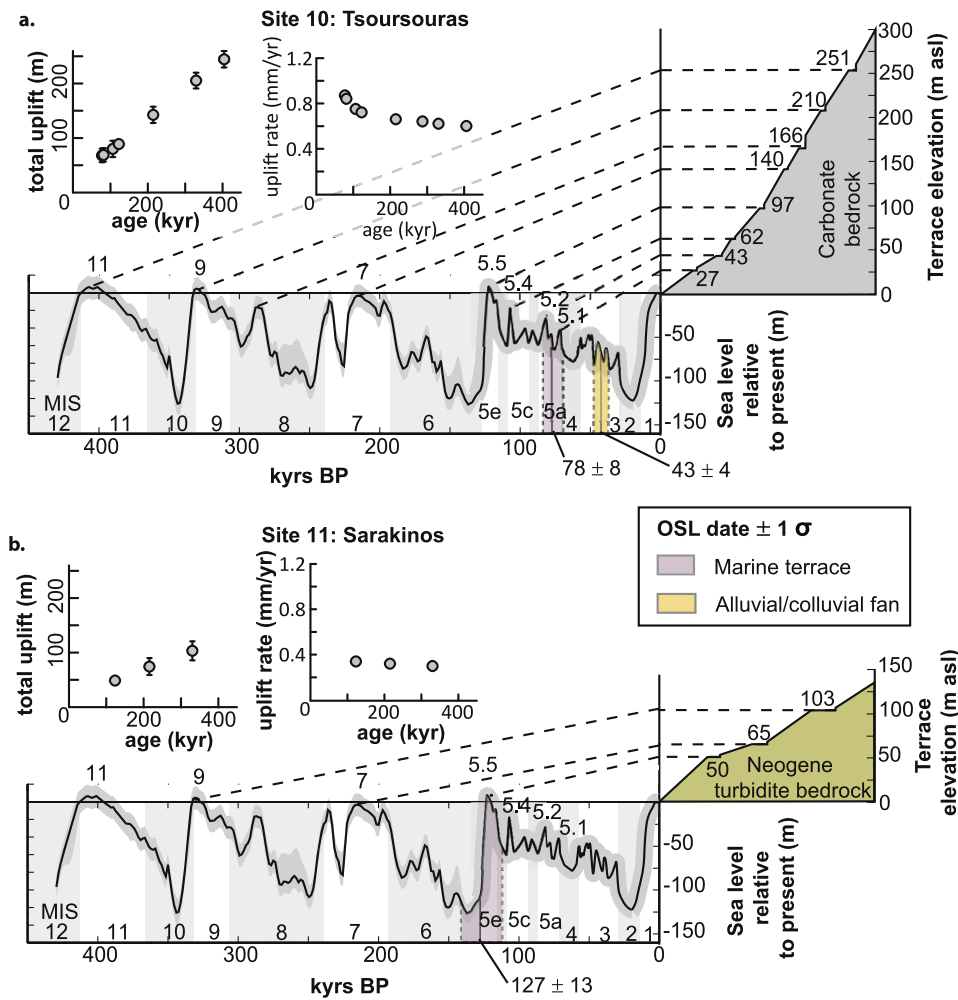


Fig. 5. Correlation of the Tsoutsouros (a – site 10) and Sarakinos (b – site 11) terrace sequences to the Late Quaternary global sea level curve. The 0 to 125 kyr sea level curve was compiled from Lambeck and Chappell (2001), while the 125 to 450 kyr segment is from Waelbroeck et al. (2002). Marine isotope stage (MIS) boundaries are from Lisiecki and Raymo (2005). Each terrace sequence is anchored to the sea level curve with an optically simulated luminescence (OSL) burial age of fine sand collected from marine terrace deposits. The Tsoutsouros sequence shows the OSL age of an alluvial fan overlying the lowest terrace in the sequence. Inset diagrams show the total uplift versus estimated terrace age with standard (68%) uncertainties on left and uplift rates for individual terraces versus assigned terrace age determined using Eqs. (1) and (2) on the right. Associated uncertainties on points lacking error bars are smaller than the symbols at the scale of these diagrams.

is preserved, with terraces spaced between 0 and 94 m amsl (Fig. 3a). The lowest terrace in this sequence is laterally extensive and buried by a thick (>3 m) Unit 1 alluvial fan. The lowest terrace is at a maximum elevation of 19 m amsl at the Lentas fault, tilts to the west, and can be traced for ~10 km before it is no longer preserved due to bedrock mass-wasting between field sites 2 and 3 (Fig. 3a). The western-most marine terraces are found near Kali Limenes, where the higher terraces are mantled by a Unit 2A alluvial fan (Fig. 3 – site 2). At the western end of the Asterousia (site 1), the shore exhibits a highly indented coastal morphology indicative of drowned river valleys, marine terraces are not preserved, and submerged Roman-era structures have been identified (Mourtzas, 1988, 2012; Peterek and Schwarze, 2004). This evidence indicates long-term stability or subsidence of this section of coast, at least during the late Holocene.

The Asterousia block has the greatest numbers and highest terrace elevations along the south-central coastline (Fig. 3b). The lowest terrace from this sequence can be traced continuously from the Lentas fault to the South-Central Crete fault as it increases in height from 4 to 25 m amsl. It is everywhere buried by a Unit 1 alluvial fan (Fig. 3b). Higher terraces are generally less prominent, with the exception of the fourth highest terrace, which is identifiable continuously for 30 km to the west of the South-Central Crete

fault (Fig. 3b). All terraces of the Asterousia block exhibit an eastward increase in elevation and inter-terrace spacing, away from the Lentas fault.

Terraces preserved in the hanging wall of the South-Central Crete fault are distinct in form and number in comparison to those in the adjacent footwall (site 10 – Figs. 3c, 4b, c). Hanging wall terraces are broad, slope gently seaward, and are typically developed in a sequence of three. These terraces are dissected where streams drain the Dikti range front, yet can be traced for tens of kilometers along the coastline between Tsoutsouros and Tertsa (sites 11 to 17). The terraces decline in elevation from Tsoutsouros (site 11) to Arvi (site 15), at which point they increase in elevation until they are truncated by the NE-SW striking Ierapetra fault (Fig. 3c; Angelier, 1979; Gaki-Papanastassiou et al., 2009).

4.3. Geochronology

We report five new OSL age-dates from south-central Crete, two from alluvial fans (Fig. 3a, b – sites 4 and 8), two from the lowest terrace in the Asterousia fault block (Fig. 3b – sites 8 and 10) and one from the lowest terrace in the hanging wall of the South-Central Crete fault (Fig. 3c – site 12; for details on geochronology see Supplementary Table 2S). Two OSL samples were obtained from alluvial fan sediments burying the lowest marine terrace on

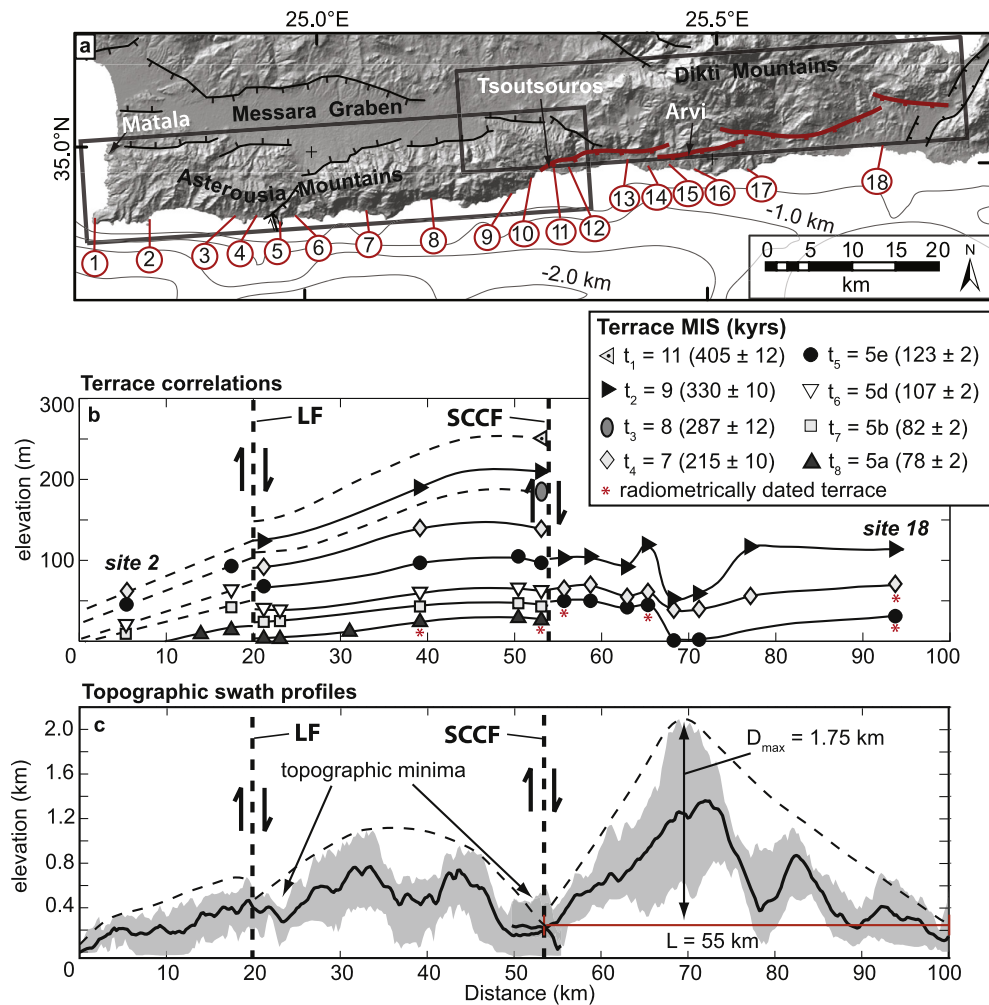


Fig. 6. (a) Map of south-central Crete identifying study site locations and swath topographic profiles shown in (d). (b) Terrace correlations for the south-central coastline of Crete. (c) Swath profiles taken along the Asterousia and Dikti Mountains. Dashed lines indicate the profile of maximum displacement as determined by correlation of the highest peaks in the respective fault blocks. Horizontal red line indicates the approximate elevation and length (L) of the South-Central Crete fault and the vertical line with black arrows shows the maximum footwall displacement (D_{max}). The ratio of maximum displacement to fault length is 0.032. Vertical bold-dashed lines in **b** & **c** show the location where the Lentas Fault (LF) and South-Central Crete fault (SCCF) intersect the shore. See supplemental Tables 2S and 3S for additional terrace geochronologic results. (For interpretation of the references to color in this figure legend, the reader is referred to the web version of this article.)

either side of the Lentas Fault at sites 4 and 8. The burial ages (with associated standard errors) of 40.8 ± 3.2 and 37.5 ± 3.1 kyr respectively, are consistent with fan aggradation during lower sea levels of MIS 3.

The lowest marine terrace in the Asterousia block is continuously exposed for >30 km along the coastline between sites 5 and 10; as such it a robust feature for tying other terraces to the eustatic curve (see Section 5.2). Two OSL samples were collected from the lowest terrace at sites 8 and 10 and have burial ages (with associated standard errors) of 78 ± 8 kyr and 72 ± 8 kyr, respectively. These OSL ages indicate that the lowest terrace in the Asterousia block was cut and deposited during the MIS 5a sea-level highstand (Supplementary Table 2S).

Stratified sediments immediately above the bedrock strath from the lowest marine terrace in the hanging wall of the South-Central Crete fault 2.5 km east of Tsoutsouros (site 12) have an OSL age of 127 ± 13 kyr. This date supports earlier geochronology based upon index fossils (*Strombus bubonius*) and shell $^{230}\text{Th}/^{235}\text{U}$ and $^{231}\text{Pa}/^{235}\text{U}$ age-dates of various fauna extracted from the two lowest terraces on the South-Central Crete fault hanging wall block at sites 14 and 18 (Supplementary Tables 2S, 3S; Angelier, 1979). These results demonstrate that the lowest preserved terrace in the

hanging wall of the South-Central Crete fault was emplaced during the last full interglacial (MIS 5e) sea-level highstand at ~ 123 kyr.

5. Discussion

5.1. Coastal chronostratigraphy

Geochronologic results from the lowest marine terraces in the Asterousia fault block and from the hanging wall of the South-Central Crete fault are consistent with terrace emplacement during eustatic highstands (Fig. 5). Locally, marine terraces exhibit beach facies sands and gravels that are capped by shallow algal reef deposits suggesting strath cutting and sediment deposition during sea level transgression-to-highstand phases (Supplementary Fig. 1S).

Absolute and relative geochronologic results allow for the constraint of alluvial fan deposition (Fig. 5a). Unit 1 fans were deposited during lower than modern sea level conditions associated with MIS 3. Soil development indicates that Unit 1 fans are relatively younger than Unit 2 fans, which unconformably overlie MIS 5 marine terraces (see Section 5.2). This evidence combined the Unit 1–2A inset topographic relationship and the observation of lower base level during alluvial fan deposition suggests that both

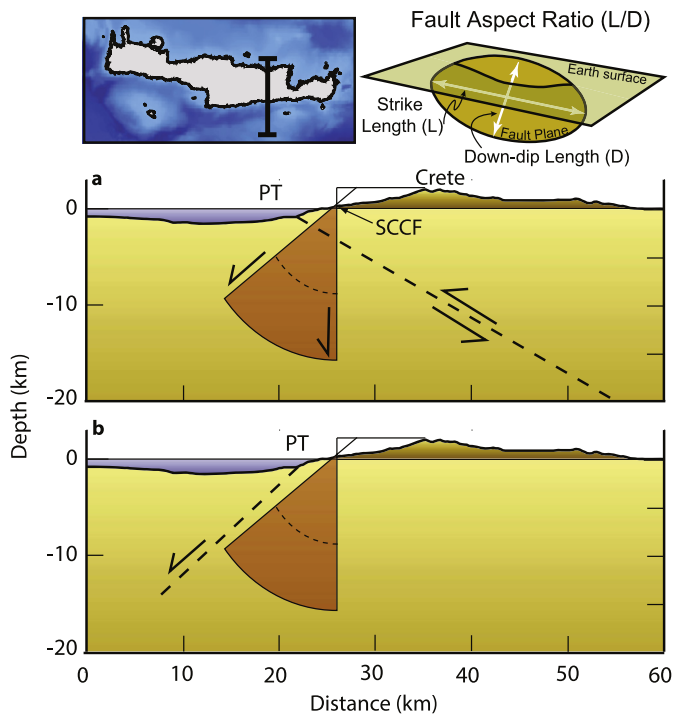


Fig. 7. Top left. Map showing the location of the topographic and upper crustal cross-section in panels **a** and **b**, portrayed with no vertical exaggeration. Top right. Schematic showing fault aspect ratio dimensions. **(a)** Geometry of the South-Central Crete fault (SCCF) in cross-section, determined using probable and measured fault plane dip angles (40° to 90°) and fault aspect ratios with respect to the proposed orientation of a 30° north-dipping Ptolemy Trough thrust fault (PT). This interpretation of the Ptolemy fault is based on five steeply-dipping contractional focal mechanisms thought to originate in the upper crust south of the Ptolemy trough (Shaw and Jackson, 2010). This scenario is geometrically impossible with an active South-Central Crete fault and our field observations. **(b)** The South-Central Crete fault is the same as in **(a)**, but the Ptolemy fault is here shown as a 40° to 90° south-dipping extensional-to-transensional fault. This interpretation is based on data presented in this study and side-scan sonar, seismic reflection surveys, sea-floor coring and the spatial pattern of micro-earthquakes (Alves et al., 2007; Becker et al., 2010). This orientation for the Ptolemy fault is consistent with an active South-Central Crete Fault.

Units 2A and 2B fans were deposited during MIS 4. The difference in soil development between Unit 2A and 2B fans is interpreted to be function of soil parent material between the two fault blocks. Unit 2A fans are located where carbonates crop out, resulting in the development of calcic soil horizons. In contrast, Unit 2B fans are located in areas underlain by Neogene marine sediments lacking the carbonate necessary for the rapid development of calcic horizons.

In summary, marine terraces are cut and emplaced during transgression to, or during sea-level high stands and alluvial fans prograde seaward during periods of eustatic drawdown. This coastal chronostratigraphy is consistent with the general timing and eustatic-climatic correlations arrived at in previous studies of Cretan marine terraces (Angelier, 1979; Wegmann, 2008; Strasser et al., 2011) and alluvial fans (Pope et al., 2008).

5.2. Terrace correlations, fault displacements, and coastal uplift

OSL burial dating, previously published geochronology, stratigraphic and sedimentologic relationships, soil profile development and the physical continuity of terraces along the coastline allows us to anchor terrace sequences to the Quaternary eustatic curve at 18 sites (Figs. 5, 6). While room exists to correlate individual terraces from a given sequence to slightly older or younger eustatic peaks, such interpretations cause little change in the total magnitude and derived uplift rates. Our preferred correlations are those

that yield the simplest, least-varying trend of long-term coastal uplift. For example, the west Tsoutsouros sequence (site 10) contains the greatest number of terraces and yields the most complete record of coastal uplift along the entire south coast of Crete for the last 400 kyr (Figs. 4b, 5a). Every significant sea level highstand during MIS 5, with the exception of 5c, is represented in this sequence along with those that occurred during MIS 7, 8, 9 and 11. The rate of coastal uplift has steadily increased through time at nearly every site across multiple terrace tie-points.

Our field investigations unambiguously demonstrate that the Lentas and South-Central Crete faults are active as they offset middle-to-late Pleistocene marine terraces and alluvial fans. The Quaternary throw rate for the Lentas and South-Central Crete faults is near time-constant, averaging 0.2 and 0.35 m kyr^{-1} , respectively. This result is direct evidence that N-S oriented extension is active in southern Crete, consistent with some focal mechanisms derived from shallow offshore earthquakes sourced a few kilometers to the south (Nyst and Thatcher, 2004; Bohnhoff et al., 2005). Furthermore, marine terraces are preserved in the footwalls and hanging walls of these active faults, demanding that regional uplift persists despite active margin-normal extension.

The gentle westward tilt of marine terraces and eastward increase in terrace elevation spacing observed in the Lentas and Asterousia blocks is indicative of characteristic earthquake ruptures on the two offshore range-front faults (Fig. 6b; e.g. Schwartz and Coppersmith, 1984). The average rate of late Quaternary surface uplift along the Lentas block varies from 0 to 0.8 m kyr^{-1} , whereas along the Asterousia block it is somewhat faster, between 0.5 to 1 m kyr^{-1} . These rates are slightly lower, but comparable to the late Pleistocene uplift rates of southwestern Crete, to the west of the Messara plain (Wegmann, 2008; Strasser et al., 2011).

The Lentas and South-Central Crete faults extend offshore and almost certainly form the subaqueous range-bounding structures of the Lentas and Asterousia fault blocks (Fig. 6). Side-scan sonar, seismic reflection, and sea-floor cores identify the subaqueous range front fault of the Lentas block as a south-dipping extensional structure supporting this interpretation (Alves et al., 2007). The Lentas and South-Central Crete faults are the onshore extension of south-dipping faults related to the construction of the Asterousia Mountains and Ptolemy trough. Rough estimates of the size of these faults suggest they could generate earthquakes as large as M_w 6.5 (Wells and Coppersmith, 1994).

The elevations of the hanging wall terraces, east of Tsoutsouros, are more variable relative to the other fault blocks, yet a gentle anticlinal warping is observed (Fig. 6). Local variability in terrace elevations is due to slip on small N-S striking subsidiary faults embedded in the hanging wall. The broad down warping of the terraces is consistent with models of fault displacement for single or mechanically linked faults (e.g. Cartwright et al., 1995). Average rates of uplift from the hanging wall range between 0.1 and 0.4 m kyr^{-1} , consistent with previous studies of the marine terraces between Tsoutsouros and Irapetra (Angelier, 1979; Gaki-Papanastassiou et al., 2009). These uplift rates are slightly faster than those derived from Pliocene marine faunal assemblages (0.1 – 0.2 m kyr^{-1}) preserved in turbidites now exposed along the hanging wall of the South-Central Crete fault (Zachariasse et al., 2008). Taken together these findings demonstrate that coastal uplift in south central Crete is the culmination of localized slip along south-dipping normal faults superimposed upon regional uplift.

5.3. Kinematics of the Ptolemy trough fault

The finding that the footwalls and hanging walls of active normal faults are rising above sea level in south-central Crete is relevant to the ongoing debate over the topographic and geodynamic evolution of the Hellenic forearc. Two alternative explana-

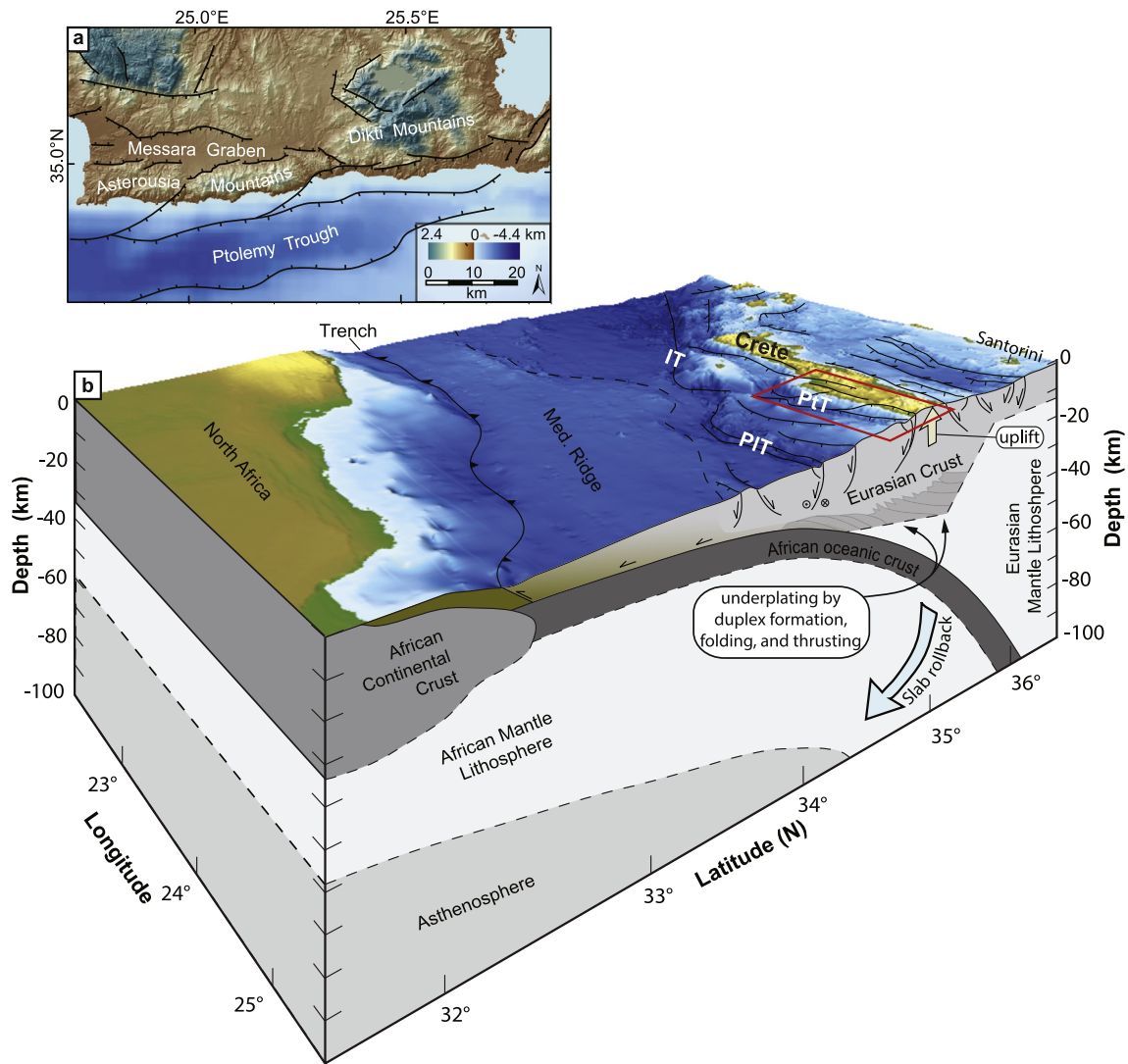


Fig. 8. (a) Map view of the study area showing our interpretation of the linkage between on-and-offshore faults. The Ptolemy trough is interpreted to be a graben structure, similar to the onshore Messara Graben north of the Asterousia Mountains. Fault teeth are on the hanging wall. Red box outlines the location of map in a projected onto the regional map and cross section in b. (b) Northwest-oriented perspective view of regional topography, crust, and upper mantle structure. The crust and mantle sections are modified from Gudmundsson and Sambridge (1998) and Meier et al. (2004). The Ionian (IT), Ptolemy (PtT), and Pliny (PIT) troughs are labeled. Based on the results of our study, we propose that convergence is accommodated in the deep crust by duplex formation, folding and thrusting that thickens the crust, which drives regional uplift at the Earth's surface and is accompanied by extension in the upper portions of the wedge (e.g. Angelier et al., 1982; Platt, 1986). (For interpretation of the references to color in this figure legend, the reader is referred to the web version of this article.)

tions could explain sustained simultaneous uplift and extension: (1) the active normal faults are superficial, developing in response to anticlinal folding above a north-dipping splay thrust that daylights in the Ptolemy trough about 10 km to the south (Meulenkamp et al., 1988, 1994; Taymaz et al., 1990; Jackson, 1994; Shaw and Jackson, 2010); or (2) the Ptolemy trough fault is synthetic to, and linked with onshore structures implying that margin-normal (N–S) extension is regional and has continued into the Quaternary (Angelier, 1979; Angelier et al., 1982; Ring et al., 2001; Peterek and Schwarze, 2004). Field mapping, the pattern of coastal uplift and marine geophysical datasets suggest that the Lentas and South–Central Crete faults are the onshore expressions of the Ptolemy fault (Alves et al., 2007). To strengthen this interpretation we use geometric reconstructions to show that activity of the South–Central Crete fault is only consistent with a synthetic structure in the Ptolemy trough.

Displacement patterns observed along the ~55 km long South–Central Crete fault array suggest that its individual fault segments are kinematically linked at depth. First, the broad anticlinal warp-

ing of terraces is consistent with expectations for displacement on a linked fault array (Fig. 6b). Second, the pattern and magnitude of displacement in the footwall, estimated from the topographic envelope of the Dikti Mountains (cf. Anders and Schlische, 1994; Hetzel et al., 2004), matches empirical and theoretical predictions for displacement on a kinematically linked fault (Fig. 6c). Linked faults will have a single centrally located maximum in the footwall displacement profile, while unlinked structures will have multiple maxima; the South–Central Crete fault falls into the former category (Dawers et al., 1993; Cartwright et al., 1995; Dawers and Anders, 1995; Manighetti et al., 2001, 2005). Further, the ratio of maximum fault displacement to fault surface length for the South–Central Crete fault is 0.032, consistent with predicted ratios for linked structures of ~0.03 (Fig. 6c; Dawers et al., 1993; Schlische et al., 1996).

Observations supporting a mechanically linked South–Central Crete fault permit use of fault aspect ratios (a fault's strike-length to down-dip length) to estimate first-order fault dimensions for geometric reconstructions. Linked faults that are mechanically un-

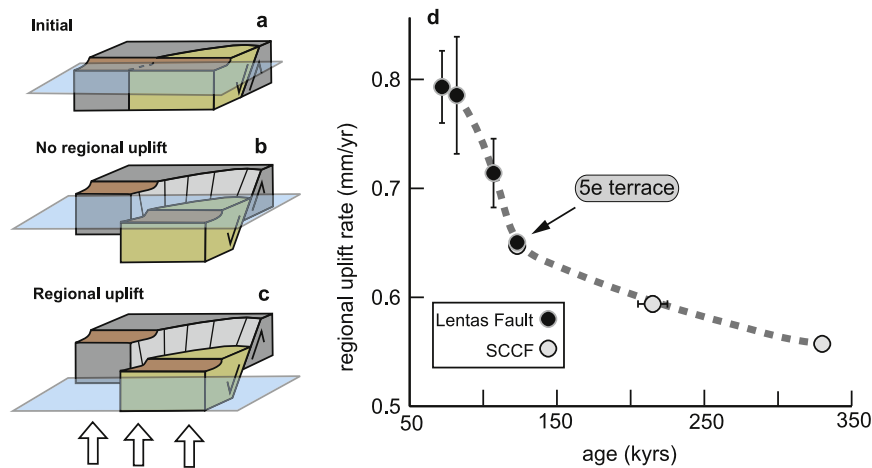


Fig. 9. Schematic illustration of a faulted marine terrace that is also affected by regional uplift and assuming constant sea level. (a) Terrace is initially cut across the fault. (b) One or more fault ruptures separate the terrace. Terrace uplift in the footwall is $\sim 20\%$ of fault displacement, while terrace subsidence in the hanging wall accounts for the other $\sim 80\%$ of fault displacement (e.g. Stein et al., 1988). (c) Regional uplift raises both foot- and hanging walls above sea level. (d) The results of this analysis applied to the Lentas and South-Central Crete faults, which reveal an increasing rate of regional uplift during the middle-to-late Quaternary. Confidence in this analysis is provided by the uplift rates derived from the 123 kyr 5e marine terrace offset by each fault and that are statistically the same. This signal of uplift is interpreted as the result of deep underplating along the subduction interface.

restricted exhibit aspect ratios between 1 and 5 (Fig. 7; Nicol et al., 1996; Willemse et al., 1996; Willemse, 1997; Soliva and Benedicto, 2005; Soliva et al., 2006). Using fault aspect ratios between 3 and 5, we derive a conservative estimate for the down-dip length of the South-Central Crete fault to between 11 and 18 km. This reconstruction predicts that the fault extends 5 to 16 km beneath the surface, depending on the assigned dip angle (40° to 90°) and aspect ratio (Fig. 7). Importantly, these are likely minimum estimates of fault depth because we utilize the surface length of the fault, rather than the total strike length in estimating the faults down-dip dimensions (Fig. 7). We conclude that the South-Central Crete fault is an important deep-seated structure that extends down to near the regional brittle-ductile transition (15 to 20 km; e.g. Becker et al., 2006), consistent with the pattern of micro-earthquakes south of Crete (Becker et al., 2010).

Only a south-dipping Ptolemy fault is consistent with reconstructions of the South-Central Crete fault (Fig. 7c). All other geometries result in the cross-cutting of the South-Central Crete and Ptolemy faults at depth (Fig. 7b; Meulenkamp et al., 1988, 1994; Taymaz et al., 1990; Jackson, 1994; Shaw and Jackson, 2010). Such scenarios are geometrically impossible as they require both faults to be active at the same time (e.g. Scholz and Contreras, 1998). Thus, the segment of the Ptolemy fault south of the Dikti Mountains is synthetic to the active South-Central Crete fault.

5.4. Implications for the active tectonics and geodynamics of the Hellenic subduction zone

Our results demonstrate that margin-normal extension has continued in the Central Hellenic margin throughout the Quaternary. Thus, the Asterousia and Dikti mountains should be viewed as a horst with the Ptolemy trough as a graben or half graben (Fig. 8a). Similar arguments can be extended elsewhere on Crete based on the observed association between E–W striking faults and dramatic topographic relief (Figs. 2, 8). For example, field investigations suggest that the south-dipping northern boundary fault of the Messara graben and range front of the Psiloritis Mountains accommodates extensional displacement (Fig. 7; Peterek and Schwarze, 2004; Zachariasse et al., 2011). Geophysical and coring studies show that this fault continues westward offshore forming the subaqueous range front of the Lefka Ori in southwestern Crete (Alves et al., 2007). These observations suggest that the bathymetric trough that lies south of western Crete is the submarine extension of

the Messara graben (Fig. 2). Moreover, the observation of high topography (Asterousia, Dikti, Psiloritis, Lefka Ori) in the footwalls of these faults indicates significant and fundamentally important vertical displacements. Some researchers point out the potential kinematic importance of left-lateral motion on these range bounding faults (e.g., ten Veen and Kleinspehn, 2003). We do not debate the potential for oblique motion on these structures; however, our results and those of others (e.g. Ring et al., 2001, 2003; Peterek and Schwarze, 2004) suggest that the predominant sense of motion on large E–W striking faults in the Central Hellenic forearc is dip-slip.

Our observations are incompatible with the splay thrust model of forearc growth (Meulenkamp et al., 1988, 1994; Taymaz et al., 1990; Jackson, 1994; Shaw and Jackson, 2010). The closest candidates for upper-crustal thrust or reverse faults are the Ionian and Pliny troughs, although the kinematics of these structures is debated (Fig. 1; Angelier et al., 1982; Meulenkamp et al., 1988, 1994; Taymaz et al., 1990; Jackson, 1994; Bohnhoff et al., 2001; ten Veen and Kleinspehn, 2003; Meier et al., 2007; Becker et al., 2010; Shaw and Jackson, 2010; Özbakır et al., 2013). Our findings support the interpretation that these are normal faults with perhaps some sense of oblique motion (Fig. 8b). Regardless of their kinematics, displacements along these faults will result in negligible vertical motion on Crete some 75 to 100 km northward. Our observations combine with those of previous researchers illustrate Crete is characterized active margin-normal and margin-parallel extension and ongoing uplift (Angelier et al., 1982; Ring et al., 2001; Bohnhoff et al., 2005; Caputo et al., 2006). These observations are best described by models of forearc growth in a viscous orogenic wedge, where material underplating occurs at the base of the wedge and multi-directional extension takes place in the upper crust to maintain stability (Fig. 8b; Cowan and Silling, 1978; Angelier et al., 1982; Platt, 1986; Knapmeyer and Harjes, 2000; Ring and Layer, 2003).

A temporal record of the direction, magnitude and pace of regional uplift in the absence of local extension can be determined from marine terraces offset by the Lentas and South-Central Crete faults. By ascertaining the elevations of terraces relative to sea level at the time of terrace formation, and by assuming that the displacement across an active extensional fault is partitioned over geologic time into 80% hanging wall subsidence and 20% footwall uplift (e.g. Stein et al., 1988), predicted elevations can be compared to the present-day terrace elevations to derive the regional

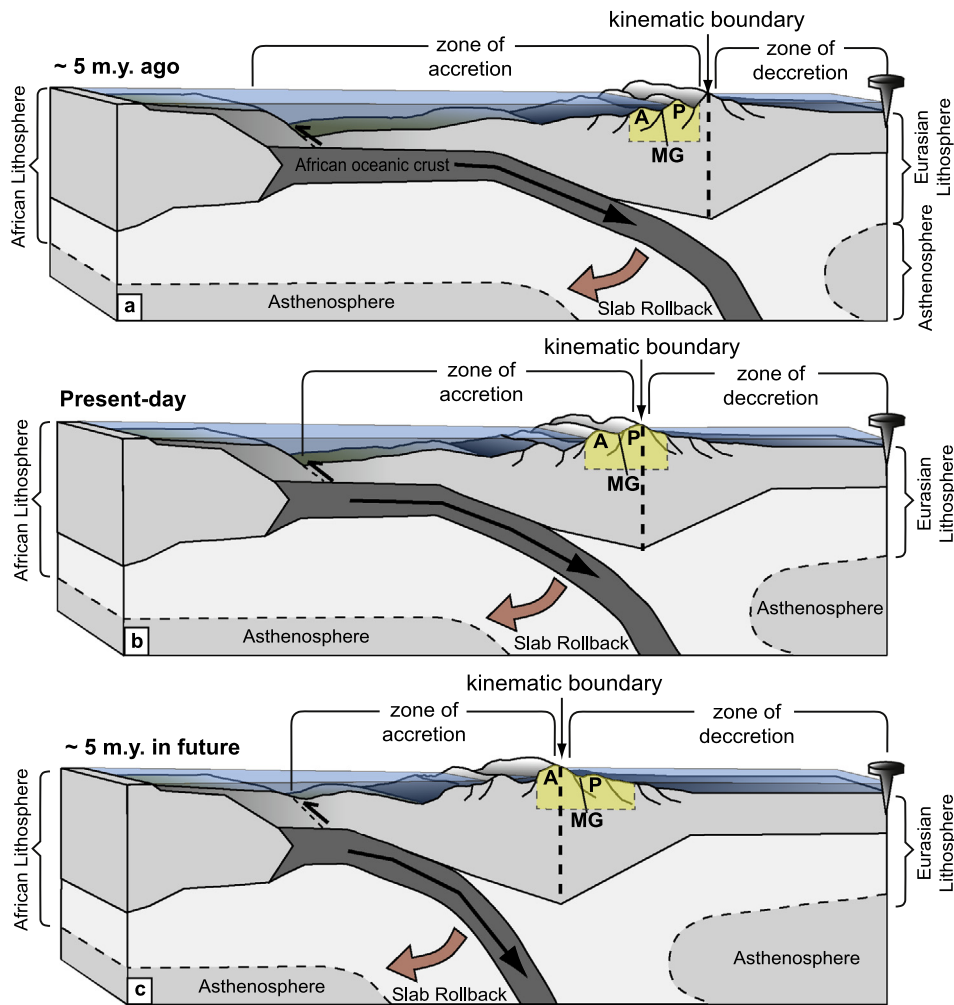


Fig. 10. Conceptual geodynamic model for the late Cenozoic evolution of the Hellenic Subduction zone. Crete (highlighted dashed box) is envisioned as a parcel of material passing through a southward migrating orogenic wave. (a) In the past (~ 5 Ma), the rocks comprising modern-day Crete occupied a position south of the apex of the orogen allowing the Messara graben and other adjacent forearc basins to fill with Neogene turbidites. (b) Crete was subsequently uplifted as the orogenic wave propagated southward and earlier topographic highs were laterally extended and decreted to the north into the Aegean Sea. (c) In the future (~ 5 Ma) the Asterousia Mountains (A) and Ptolemy Trough may occupy similar topographic positions to the present-day Psiloritis (P) Mountains and Messara Graben (MG), respectively, which may now be extended and decreted north of the kinematic boundary of the orogen. This model is based on tectonic reconstructions that show the subduction zone as a southward migrating “orogenic wave” and provides the framework from which to explain the increasing rates of regional uplift over the late Quaternary when tectonic rates of convergence and subduction have remained approximately constant.

Quaternary record of uplift from ~ 72 to 305 kyr before present (Fig. 9). Our analysis suggests that the rate of regional uplift has increased about 60% over this interval from 0.5 to 0.8 mkyr^{-1} (Fig. 9d). Rates of crustal thickening must be 3.1 to 4.3 mkyr^{-1} , assuming pure Airy isostasy and average densities for the crust and upper mantle of 2700 and 3300 kgm^{-3} , respectively. This record of uplift is similar to increasing rates of uplift inferred from marine terraces preserved to the west and east of central Crete, suggesting it is a regional phenomenon (Wegmann, 2008; Strasser et al., 2011; Strobl et al., in press). Benthic faunal assemblages preserved in Neogene marine sediments located in the Messara and Heraklion basins in central Crete and the hanging wall of the South–Central Crete fault indicate time-average uplift rates of ~ 0.20 mkyr^{-1} since the Pliocene (van Hinsbergen and Meulenkamp, 2006; Zachariasse et al., 2008, 2011). A study of the uplift history of Crete deduced from inverse modeling of longitudinal river profiles suggests uplift rates have generally increased since ~ 2 Ma (Roberts et al., 2013). Collectively, these data support a regional and increasing rate of surface uplift for what is now southern Crete throughout the late Cenozoic.

The amount of convergence and subduction velocity between the African and Eurasian plates has remained approximately steady

during the late Cenozoic (e.g. Faccenna et al., 2003; Jolivet and Brun, 2010; Ring et al., 2010). Therefore, changes in horizontal tectonic velocities are unlikely to have driven increases in Cretan surface uplift rates. Viewing Crete from a Euclidian perspective with respect to a southward migrating subduction trench provides a convenient means of understanding the history of vertical tectonics. Crete is envisioned as a “rock parcel” moving horizontally through the orogen. In this view, vertical surface motions at a given location are a reflection of changes in its horizontal position relative to a southward propagating orogenic wave (Fig. 10). A parcel of material moving through the subduction wedge will experience increasing rates of uplift before reaching the crest, or kinematic boundary of the orogenic system due to material underplating along the plate interface (Fig. 10). Today, the Lefka Ori, Psiloritis, and Dikti Mountains define the crest of the orogenic wave, demarcating the boundary between orogenic accretion in the south versus decretion – the removal of material from an orogen by lithospheric stretching and thinning – to the north (Fig. 10b).

In this conceptual model, as the orogenic wave fluxes through the material comprising present-day Crete surface uplift results due to crustal thickening induced by material underplating and the upper parts of the orogenic wedge extend in multiple directions

to maintain stability opening extensional basins (e.g., Platt, 1986). Crete occupied a subaqueous position at ~5 Ma, while topographic highs existed to the north that fed sediment into the actively opening extensional basins, such as the Messara graben (Fig. 10a; Meulenkamp et al., 1994; van Hinsbergen and Meulenkamp, 2006; Zachariasse et al., 2008, 2011). For a modern analogue to this scenario one simply needs to look 20 to 30 km south of Crete. The islands of Gavdos, Chrysi, and Koyfonisi may become the highest peaks in a large subaerial mountain range in the future, while the bathymetric lows, such as the Ptolemy trough, may become elevated forearc basins, like the Messara graben is today. The present topography of Crete may, in the future, undergo decretion to the north, as it transitions into the attenuated continental crust underlying the southward-expanding Aegean Sea (Fig. 10c).

6. Conclusions

This study of the tectonic geomorphology and structural geology of South-Central Crete allows us to draw the following conclusions:

- (1) Field mapping, absolute and relative geochronology, and correlations to Quaternary sea-levels demarcate a coastal chronostratigraphy where marine terraces are cut and emplaced during warmer intervals associated with transgressive-to-highstand sea levels, and alluvial fans prograde seaward during regressive-to-low stand eustatic intervals.
- (2) The southern coast of central Crete consists of three fault-bound blocks, each with an independent uplift history, separated by two active south-dipping normal faults.
- (3) Regional surface uplift occurs despite active margin-normal (N-S) extension, evidenced by uplifted marine terraces in the footwalls and hanging walls of active extensional faults.
- (4) Field observations and geometric reconstructions of onshore faults are incompatible with contractional faulting in the adjacent Ptolemy trough, but are consistent with a synthetic offshore extensional fault. Active margin-normal extension and regional surface uplift, likely driven by material underplating, are important processes controlling topographic development in the Hellenic forearc (e.g. Angelier et al., 1982; Platt, 1986).
- (5) The faults that bound the coastline of south-central Crete are active and pose an important seismic (and tsunami) hazard to the population centers of southern Crete and the eastern Mediterranean; however, the potential hazards associated with these faults is significantly less than suggested by researchers that favor contractional faulting astride Crete's southern coastlines (e.g. Stiros, 2010; Shaw and Jackson, 2010).
- (6) Regional uplift rates in the absence of local extension increase 60% from 0.5 to 0.8 mkyr⁻¹ during the past 300 kyr. Increasing uplift rates are observed elsewhere on Crete and may extend back into the Neogene.
- (7) We propose a simple conceptual framework for interpreting the vertical tectonic history of Crete during the late Cenozoic in which the present-day island represents the apex of an orogenic wave that is propagating south with respect to stable Eurasia, as part of a syn-convergent extensional forearc system.

Acknowledgements

Acknowledgment is made to the Donors of the American Chemical Society Petroleum Research Fund for primary support of this research under grant #50792-DN18 to Wegmann. Additional support was provided by NSF – Continental Dynamics program awards 0207980 and 0208652 to Pazzaglia and Brandon, respectively.

Gallen was supported directly by a 2011 Geological Society of America Graduate Student Research Grant (number 9596-11) and a 2012 Sigma Xi Grant-in-Aid of Research. We acknowledge the Greek Institute of Geology and Mineral Exploration for granting permission to carry out field work on Crete. Formal reviews by Douwe van Hinsbergen and Uwe Ring assisted in improving the manuscript. Discussions and reviews of an earlier version of this research by James Hibbard and Elana Leithold are also acknowledged and appreciated.

Appendix A. Supplementary material

Supplementary material related to this article can be found online at <http://dx.doi.org/10.1016/j.epsl.2014.04.038>.

References

- Alves, T., Lykousis, V., Sakellariou, D., Alexandri, S., Nomikou, P., 2007. Constraining the origin and evolution of confined turbidite systems: southern Cretan margin, Eastern Mediterranean Sea (34°30–36° N). *Geo Mar. Lett.* 27, 41–61.
- Anders, M.H., Schlische, R.W., 1994. Overlapping faults, intrabasin highs, and the growth of normal faults. *J. Geol.* 102, 165.
- Angelier, J., 1979. Recent Quaternary tectonics in the Hellenic arc; examples of geological observations on land; recent crustal movements. *Tectonophysics* 52, 267–275.
- Angelier, J., Lybérís, N., Pichon, X.L., Barrier, E., Huchon, P., 1982. The tectonic development of the Hellenic arc and the Sea of Crete: a synthesis. *Tectonophysics* 86, 159–196.
- Becker, D., Meier, T., Rische, M., Bohnhoff, M., Harjes, H.-P., 2006. Spatio-temporal microseismicity clustering in the Cretan region. *Tectonophysics* 423, 3–16.
- Becker, D., Meier, T., Bohnhoff, M., Harjes, H.P., 2010. Seismicity at the convergent plate boundary offshore Crete, Greece, observed by an amphibian network. *J. Seismol.* 14, 369–392. <http://dx.doi.org/10.1007/s10950-009-9170-2>.
- Bennett, R.A., Serpelloni, E., Hreinsdóttir, S., Brandon, M.T., Buble, G., Basic, T., Casale, G., Cavaliere, A., Anzidei, M., Marjonovic, M., Minelli, G., Molli, G., Montanari, A., 2012. Syn-convergent extension observed using the RETREAT GPS network, northern Apennines, Italy. *J. Geophys. Res., Solid Earth* 117, B04408. <http://dx.doi.org/10.1029/2011JB008744>.
- Birkeland, P.W., 1984. *Soils and Geomorphology*. Oxford University Press.
- Bohnhoff, M., Makris, J., Papanikolaou, D., Stavrakakis, G., 2001. Crustal investigation of the Hellenic subduction zone using wide aperture seismic data. *Tectonophysics* 343, 239–262.
- Bohnhoff, M., Harjes, H.-P., Meier, T., 2005. Deformation and stress regimes in the Hellenic subduction zone from focal mechanisms. *J. Seismol.* 9, 341–366.
- Brix, M.R., Stöckhert, B., Seidel, E., Theye, T., Thomson, S.N., Küster, M., 2002. Thermobarometric data from a fossil zircon partial annealing zone in high pressure-low temperature rocks of eastern and central Crete, Greece. *Tectonophysics* 349, 309–326. [http://dx.doi.org/10.1016/S0040-1951\(02\)00059-8](http://dx.doi.org/10.1016/S0040-1951(02)00059-8).
- Brun, J.-P., Sokoutis, D., 2007. Kinematics of the Southern Rhodope Core Complex (North Greece). *Int. J. Earth Sci.* 96, 1079–1099. <http://dx.doi.org/10.1007/s00531-007-0174-2>.
- Brun, J.-P., Sokoutis, D., 2010. 45 m.y. of Aegean crust and mantle flow driven by trench retreat. *Geology* 38, 815–818. <http://dx.doi.org/10.1130/g30950.1>.
- Caputo, R., Monaco, C., Tortorici, L., 2006. Multiseismic cycle deformation rates from Holocene normal fault scarps on Crete (Greece). *Terra Nova* 18, 181–190.
- Cartwright, J.A., Trudgill, B.D., Mansfield, C.S., 1995. Fault growth by segment linkage: an explanation for scatter in maximum displacement and trace length data from the Canyonlands Grabens of SE Utah. *J. Struct. Geol.* 17, 1319–1326.
- Chamot-Rooke, N., Rangin, C., Le Pichon, X., D.w. group, 2005. DOTMED: deep offshore tectonics of the Mediterranean. In: *Les Mémoires de la Société Géologique de France*, vol. 177, 64 pp.
- Cowan, D.S., Silling, R.M., 1978. A dynamic, scaled model of accretion at trenches and its implications for the tectonic evolution of subduction complexes. *J. Geophys. Res., Solid Earth* 83, 5389–5396. <http://dx.doi.org/10.1029/JB083iB11p05389>.
- Dawers, N.H., Anders, M.H., 1995. Displacement-length scaling and fault linkage. *J. Struct. Geol.* 17, 607–614.
- Dawers, N.H., Anders, M.H., Scholz, C.H., 1993. Growth of normal faults: displacement-length scaling. *Geology* 21, 1107–1110. [http://dx.doi.org/10.1130/0091-7613\(1993\)021<1107:gonfd>2.3.co;2](http://dx.doi.org/10.1130/0091-7613(1993)021<1107:gonfd>2.3.co;2).
- Faccenna, C., Jolivet, L., Piromallo, C., Morelli, A., 2003. Subduction and the depth of convection in the Mediterranean mantle. *J. Geophys. Res.* 108, 2099. <http://dx.doi.org/10.1029/2001jb001690>.
- Fassoulas, C., 2001. The tectonic development of a Neogene basin at the leading edge of the active European margin: the Heraklion basin, Crete, Greece. *J. Geodyn.* 31, 49–70.

- Fassoulas, C., Kiliyas, A., Mountrakis, D., 1994. Postnappe stacking extension and exhumation of high-pressure/low-temperature rocks in the island of Crete, Greece. *Tectonics* 13, 125–138.
- Fleming, N.C., 1978. Holocene eustatic changes and coastal tectonics in the north-east Mediterranean: implications for models of crustal consumption. *Philos. Trans. R. Soc. Lond. Ser. A, Math. Phys. Sci.* 289, 405–458.
- Gaki-Papanastassiou, K., Karymbalis, E., Papanastassiou, D., Maroukian, H., 2009. Quaternary marine terraces as indicators of neotectonic activity of the Ierapetra normal fault SE Crete (Greece). *Geomorphology* 104, 38–46.
- Gallen, S.F., 2013. The development of topography in ancient and active orogens: case studies of landscape evolution in the Southern Appalachians, USA and Crete, Greece. Ph.D. North Carolina State University, Raleigh, 171 pp.
- Georgiev, N., Pleuger, J., Froitzheim, N., Sarov, S., Jahn-Awe, S., Nagel, T.J., 2010. Separate Eocene–Early Oligocene and Miocene stages of extension and core complex formation in the Western Rhodopes, Mesta Basin, and Pirin Mountains (Bulgaria). *Tectonophysics* 487, 59–84. <http://dx.doi.org/10.1016/j.tecto.2010.03.009>.
- Gudmundsson, O., Sambridge, M., 1998. A regionalized upper mantle (RUM) seismic model. *J. Geophys. Res., Solid Earth* 103, 7121–7136.
- Hetzl, R., Tao, M., Niedermann, S., Strecker, M.R., Ivy-Ochs, S., Kubik, P.W., Gao, B., 2004. Implications of the fault scaling law for the growth of topography: mountain ranges in the broken foreland of north–east Tibet. *Terra Nova* 16, 157–162. <http://dx.doi.org/10.1111/j.1365-3121.2004.00549.x>.
- Jackson, J., 1994. Active tectonics of the Aegean region. *Annu. Rev. Earth Planet. Sci.* 22, 239–271. <http://dx.doi.org/10.1146/annurev.ea.22.050194.001323>.
- Jolivet, L., Brun, J.-P., 2010. Cenozoic geodynamic evolution of the Aegean. *Int. J. Earth Sci.* 99, 109–138. <http://dx.doi.org/10.1007/s00531-008-0366-4>.
- Jolivet, L., Goffé, B., Monié, P., Truffert-Luxey, C., Patriat, M., Bonneau, M., 1996. Miocene detachment in Crete and exhumation P–T paths of high-pressure metamorphic rocks. *Tectonics* 15, 1129–1153.
- Kastens, K.A., 1991. Rate of outward growth of the Mediterranean ridge accretionary complex. *Tectonophysics* 199, 25–50.
- Kelletat, D., 1996. Perspectives in coastal geomorphology of western Crete, Greece. *Z. Geomorph. N.F. Suppl. Bd.* 102, 1–19.
- Knapmeyer, M., 1999. Geometry of the Aegean Benioff Zone. *Ann. Geofis.* 42, 27–38.
- Knapmeyer, M., Harjes, H.-P., 2000. Imaging crustal discontinuities and the downgoing slab beneath western Crete. *Geophys. J. Int.* 143, 1–21. <http://dx.doi.org/10.1046/j.1365-246x.2000.00197.x>.
- Kreemer, C., Chamot-Rooke, N., 2004. Contemporary kinematics of the southern Aegean and the Mediterranean Ridge. *Geophys. J. Int.* 157, 1377–1392. <http://dx.doi.org/10.1111/j.1365-246X.2004.02270.x>.
- Lajoie, K.R., 1986. Coastal tectonics. In: Wallace, R. (Ed.), *Active Tectonics. In: Studies in Geophysics Series, Geophysical Research Forum*. National Academy Press, Washington, D.C., pp. 95–124.
- Lambeck, K., Chappell, J., 2001. Sea level change through the last glacial cycle. *Science* 292, 679–686. <http://dx.doi.org/10.1126/science.1059549>.
- Le Pichon, X., Angelier, J., 1981. The Aegean Sea. *Philos. Trans. R. Soc. Lond. Ser. A, Math. Phys. Sci.* 300, 357–372.
- Liati, A., Gebauer, D., 1999. Constraining the prograde and retrograde P–T path of Eocene HP rocks by SHRIMP dating of different zircon domains: inferred rates of heating, burial, cooling and exhumation for central Rhodope, northern Greece. *Contrib. Mineral. Petrol.* 135, 340–354. <http://dx.doi.org/10.1007/s004100050516>.
- Lisiecki, L.E., Raymo, M.E., 2005. A Pliocene–Pleistocene stack of 57 globally distributed benthic $\delta^{18}\text{O}$ records. *Paleoceanography* 20, PA1003. <http://dx.doi.org/10.1029/2004pa001071>.
- Manighetti, I., King, G.C.P., Gaudemer, Y., Scholz, C.H., Doubre, C., 2001. Slip accumulation and lateral propagation of active normal faults in Afar. *J. Geophys. Res.* 106, 13667–13696. <http://dx.doi.org/10.1029/2000jb900471>.
- Manighetti, I., Campillo, M., Sammis, C., Mai, P.M., King, G., 2005. Evidence for self-similar, triangular slip distributions on earthquakes: implications for earthquake and fault mechanics. *J. Geophys. Res.* 110, B05302. <http://dx.doi.org/10.1029/2004jb003174>.
- Marsellos, A.E., Kidd, W.S.F., Garver, J.I., 2010. Extension and exhumation of the HP/LT rocks in the Hellenic forearc ridge. *Am. J. Sci.* 310, 1–36. <http://dx.doi.org/10.2475/01.2010.01>.
- McClusky, S., Balassanian, S., Barka, A., Demir, C., Ergintav, S., Georgiev, I., Gurkan, O., Hamburger, M., Hurst, K., Kahle, H., Kastens, K., Kekelidze, G., King, R., Kotzev, V., Lenk, O., Mahmoud, S., Mishin, A., Nadariya, M., Ouzounis, A., Paradissis, D., Peter, Y., Prilepin, M., Reilinger, R., Sanli, I., Seeger, H., Tealeb, A., Toksoz, M.N., Veis, G., 2000. Global positioning system constraints on plate kinematics and dynamics in the eastern Mediterranean and Caucasus. *J. Geophys. Res., Solid Earth* 105, 5695–5719.
- Meier, T., Rische, M., Endrun, B., Vafidis, A., Harjes, H.P., 2004. Seismicity of the Hellenic subduction zone in the area of western and central Crete observed by temporary local seismic networks. *Tectonophysics* 383, 149–169.
- Meier, T., Becker, D., Endrun, B., Rische, M., Bohnhoff, M., Stockhert, B., Harjes, H.-P., 2007. A model for the Hellenic subduction zone in the area of Crete based on seismological investigations. *Geol. Soc. (Lond.) Spec. Publ.* 291, 183–199. <http://dx.doi.org/10.1144/sp291.9>.
- Merritts, D., Bull, W.B., 1989. Interpreting Quaternary uplift rates at the Mendocino triple junction, northern California, from uplifted marine terraces. *Geology* 17, 1020–1024. [http://dx.doi.org/10.1130/0091-7613\(1989\)017<1020:iqurat>2.3.co;2](http://dx.doi.org/10.1130/0091-7613(1989)017<1020:iqurat>2.3.co;2).
- Meulenkamp, J.E., Wortel, M.J.R., van Wamel, W.A., Spakman, W., Hoogerduyn Stratig, E., 1988. On the Hellenic subduction zone and the geodynamic evolution of Crete since the late Middle Miocene. *Tectonophysics* 146, 203–215.
- Meulenkamp, J.E., van der Zwaan, G.J., van Wamel, W.A., 1994. On late Miocene to recent vertical motions in the Cretan segment of the Hellenic arc. *Tectonophysics* 234, 53–72.
- Mourtzas, N.D., 1988. Neotectonic evolution of Messara's Gulf – submerged archaeological constructions and use of the coast during the prehistoric and historic periods. In: Marinou, P.G., Koukis, G.C. (Eds.), *The Engineering Geology of Ancient Works, Monuments and Historical Sites – Preservation and Protection*. A.A. Balkema, Rotterdam, pp. 1565–1573.
- Mourtzas, N.D., 2012. Archaeological indicators for sea level change and coastal neotectonic deformation: the submerged Roman fish tanks of the gulf of Matala, Crete, Greece. *J. Archaeol. Sci.* 39, 884–895.
- Nicol, A., Watterson, J., Walsh, J.J., Childs, C., 1996. The shapes, major axis orientations and displacement patterns of fault surfaces. *J. Struct. Geol.* 18, 235–248.
- Nyst, M., Thatcher, W., 2004. New constraints on the active tectonic deformation of the Aegean. *J. Geophys. Res.* 109, B11406. <http://dx.doi.org/10.1029/2003jb002830>.
- Özbakır, A.D., Şengör, A.M.C., Wortel, M.J.R., Govers, R., 2013. The Pliny–Strabo trench region: a large shear zone resulting from slab tearing. *Earth Planet. Sci. Lett.* 375, 188–195.
- Papazachos, B.C., 1996. Large seismic faults in the Hellenic arc. *Ann. Geofis.* 39, 891–903.
- Papazachos, B.C., Karakostas, V.G., Papazachos, C.B., Scordilis, E.M., 2000. The geometry of the Wadati–Benioff zone and lithospheric kinematics in the Hellenic arc. *Tectonophysics* 319, 275–300.
- Pe-Piper, G., Piper, D.J.W., 2002. The Igneous Rocks of Greece: The Anatomy of an Orogen. *Gebr. Borntraeger, Berlin*.
- Pe-Piper, G., Piper, D.J.W., 2006. Unique features of the Cenozoic igneous rocks of Greece. *Spec. Pap., Geol. Soc. Am.* 409, 259–282. [http://dx.doi.org/10.1130/2006.2409\(14\)](http://dx.doi.org/10.1130/2006.2409(14)).
- Pe-Piper, G., Piper, D.J.W., 2007. Neogene backarc volcanism of the Aegean: new insights into the relationship between magmatism and tectonics. *Spec. Pap., Geol. Soc. Am.* 418, 17–31. [http://dx.doi.org/10.1130/2007.2418\(02\)](http://dx.doi.org/10.1130/2007.2418(02)).
- Peterek, A., Schwarze, J., 2004. Architecture and Late Pliocene to recent evolution of outer-arc basins of the Hellenic subduction zone (south–central Crete, Greece). *J. Geodyn.* 38, 19–55.
- Picotti, V., Pazzaglia, F.J., 2008. A new active tectonic model for the construction of the Northern Apennines mountain front near Bologna (Italy). *J. Geophys. Res., Solid Earth* 113, B08412. <http://dx.doi.org/10.1029/2007JB005307>.
- Pirazzoli, P.A., Thommeret, J., Thommeret, Y., Laborel, J., Montag-Gioni, L.F., 1982. Crustal block movements from Holocene shorelines: Crete and Antikythira (Greece). *Tectonophysics* 86, 27–43.
- Platt, J.P., 1986. Dynamics of orogenic wedges and the uplift of high-pressure metamorphic rocks. *Geol. Soc. Am. Bull.* 97, 1037–1053. [http://dx.doi.org/10.1130/0016-7606\(1986\)97<1037:doowat>2.0.co;2](http://dx.doi.org/10.1130/0016-7606(1986)97<1037:doowat>2.0.co;2).
- Pope, R., Wilkinson, K., Skourtsos, E., Triantaphyllou, M., Ferrier, G., 2008. Clarifying stages of alluvial fan evolution along the Sfakian piedmont, southern Crete: new evidence from analysis of post-incisive soils and OSL dating. *Geomorphology* 94, 206–225.
- Rahl, J.M., Anderson, K.M., Brandon, M.T., Fassoulas, C., 2005. Raman spectroscopic carbonaceous material thermometry of low-grade metamorphic rocks: calibration and application to tectonic exhumation in Crete, Greece. *Earth Planet. Sci. Lett.* 240, 339–354.
- Reilinger, R., McClusky, S., Vernant, P., Lawrence, S., Ergintav, S., Cakmak, R., Ozener, H., Kadirov, F., Guliev, I., Stepanyan, R., Nadariya, M., Hahubia, G., Mahmoud, S., Sakr, K., ArRajehi, A., Paradissis, D., Al-Aydrus, A., Prilepin, M., Guseva, T., Evren, E., Dmitrova, A., Filikov, S.V., Gomez, F., Al-Ghazzi, R., Karam, G., 2006. GPS constraints on continental deformation in the Africa–Arabia–Eurasia continental collision zone and implications for the dynamics of plate interactions. *J. Geophys. Res., Solid Earth* 111, 26. <http://dx.doi.org/10.1029/2005JB004051>.
- Rhodes, E.J., 2011. Optically stimulated luminescence dating of sediments over the Past 200,000 years. *Annu. Rev. Earth Planet. Sci.* 39, 461–488. <http://dx.doi.org/10.1146/annurev-earth-040610-133425>.
- Ring, U., LAYER, P.W., 2003. High-pressure metamorphism in the Aegean, eastern Mediterranean: underplating and exhumation from the Late Cretaceous until the Miocene to Recent above the retreating Hellenic subduction zone. *Tectonics* 22, 1022. <http://dx.doi.org/10.1029/2001TC001350>.
- Ring, U., Brachert, T., Fassoulas, C., 2001. Middle Miocene graben development in Crete and its possible relation to large-scale detachment faults in the southern Aegean. *Terra Nova* 13, 297–304. <http://dx.doi.org/10.1046/j.1365-3121.2001.00359.x>.
- Ring, U., Brachert, T.C., ten Veen, J.H., Kleinspehn, K.L., 2003. Discussion on incipient continental collision and plate-boundary curvature: Late Pliocene–Holocene transtensional Hellenic forearc, Crete, Greece. *J. Geol. Soc. (Lond.)* 160, 819–824. <http://dx.doi.org/10.1144/0016-764903-052>.

- Ring, U., Glodny, J., Will, T., Thomson, S., 2010. The Hellenic subduction system: high-pressure metamorphism, exhumation, normal faulting, and large-scale extension. *Annu. Rev. Earth Planet. Sci.* 38, 45–76. <http://dx.doi.org/10.1146/annurev.earth.050708.170910>.
- Roberts, G.G., White, N.J., Shaw, B., 2013. An uplift history of Crete, Greece, from inverse modeling of longitudinal river profiles. *Geomorphology* 198, 177–188. <http://dx.doi.org/10.1016/j.geomorph.2013.05.026>.
- Royden, L.H., 1993. The tectonic expression slab pull at continental convergent boundaries. *Tectonics* 12, 303–325. <http://dx.doi.org/10.1029/92tc02248>.
- Ryan, W.B.F., Kastens, K.A., Cita, M.B., 1982. Geological evidence concerning compressional tectonics in the eastern Mediterranean. *Tectonophysics* 86, 213–242.
- Schlische, R.W., Young, S.S., Ackermann, R.V., Gupta, A., 1996. Geometry and scaling relations of a population of very small rift-related normal faults. *Geology* 24, 683–686. [http://dx.doi.org/10.1130/0091-7613\(1996\)024<0683:gasroa>2.3.co;2](http://dx.doi.org/10.1130/0091-7613(1996)024<0683:gasroa>2.3.co;2).
- Scholz, C.H., Contreras, J.C., 1998. Mechanics of continental rift architecture. *Geology* 26, 967–970. [http://dx.doi.org/10.1130/0091-7613\(1998\)026<0967:mocra>2.3.co;2](http://dx.doi.org/10.1130/0091-7613(1998)026<0967:mocra>2.3.co;2).
- Schwartz, D.P., Coppersmith, K.J., 1984. Fault behavior and characteristic earthquakes: examples from the Wasatch and San Andreas fault zones. *J. Geophys. Res.* 89, 5681–5698. <http://dx.doi.org/10.1029/JB089iB07p05681>.
- Seidel, E., Kreuzer, H., Harre, W., 1982. A Late Oligocene/Early Miocene pressure belt in the External Hellenides. *Geol. Jahrb., Reihe E Geophys.* 23, 165–206.
- Shaw, B., Jackson, J., 2010. Earthquake mechanisms and active tectonics of the Hellenic subduction zone. *Geophys. J. Int.* 181, 966–984.
- Soliva, R., Benedicto, A., 2005. Geometry, scaling relations and spacing of vertically restricted normal faults. *J. Struct. Geol.* 27, 317–325.
- Soliva, R., Benedicto, A., Maerten, L., 2006. Spacing and linkage of confined normal faults: importance of mechanical thickness. *J. Geophys. Res.* 111, B01402. <http://dx.doi.org/10.1029/2004jb003507>.
- Spakman, W., Wortel, M.J.R., Vlaar, N.J., 1988. The Hellenic subduction zone: a tomographic image and its geodynamic implications. *Geophys. Res. Lett.* 15, 60–63. <http://dx.doi.org/10.1029/GL015i001p00060>.
- Stein, R.S., King, G.C.P., Rundle, J.B., 1988. The growth of geological structures by repeated earthquakes 2. Field examples of continental dip-slip faults. *J. Geophys. Res.* 93, 13319–13331. <http://dx.doi.org/10.1029/JB093iB11p13319>.
- Stiros, S.C., 2010. The 8.5+ magnitude, AD365 earthquake in Crete: coastal uplift, topography changes, archaeological and historical signature. *Quat. Int.* 216, 54–63.
- Strasser, T.F., Runnels, C., Wegmann, K., Panagopoulou, E., McCoy, F., Digregorio, C., Karkanas, P., Thompson, N., 2011. Dating Palaeolithic sites in southwestern Crete, Greece. *J. Quat. Sci.* 26, 553–560. <http://dx.doi.org/10.1002/jqs.1482>.
- Strobl, M., Hetzel, R., Fassoulas, C., Kubik, P.W., in press. A long-term rock uplift rate for eastern Crete and geodynamic implications for the Hellenic subduction zone. *J. Geodyn.* <http://dx.doi.org/10.1016/j.jog.2014.04.002>.
- Taymaz, T., Jackson, J.A., Westaway, R., 1990. Earthquake mechanisms in the Hellenic trench near Crete. *Geophys. J. Int.* 102, 695–731.
- ten Veen, J.H., Kleinspehn, K.L., 2003. Incipient continental collision and plate-boundary curvature: Late Pliocene–Holocene transtensional Hellenic forearc, Crete, Greece. *J. Geol. Soc. (Lond.)* 160, 161–181. <http://dx.doi.org/10.1144/0016-764902-067>.
- Theye, T., Seidel, E., 1993. Uplift-related retrogression history of aragonite marbles in Western Crete (Greece). *Contrib. Mineral. Petrol.* 114, 349–356. <http://dx.doi.org/10.1007/bf01046537>.
- Theye, T., Seidel, E., Vidal, O., 1992. Carpholite, sudoite, and chloritoid in low-grade high-pressure metapelites from Crete and the Peloponnese, Greece. *Eur. J. Mineral.* 4, 487–507.
- Thomson, S.N., Stöckhert, B., Brix, M.R., 1998. Thermochronology of the high-pressure metamorphic rocks of Crete, Greece: implications for the speed of tectonic processes. *Geology* 26, 259–262. [http://dx.doi.org/10.1130/0091-7613\(1998\)026<0259:tothpm>2.3.co;2](http://dx.doi.org/10.1130/0091-7613(1998)026<0259:tothpm>2.3.co;2).
- Thomson, S.N., Brandon, M.T., Reiners, P.W., Zattin, M., Isaacson, P.J., Balestrieri, M.L., 2010. Thermochronologic evidence for orogen-parallel variability in wedge kinematics during extending convergent orogenesis of the northern Apennines, Italy. *Geol. Soc. Am. Bull.* 122, 1160–1179. <http://dx.doi.org/10.1130/b26573.1>.
- Tomaschek, F., Kennedy, A.K., Villa, I.M., Lagos, M., Ballhaus, C., 2003. Zircons from Syros, Cyclades, Greece—recrystallization and mobilization of Zircon during high-pressure metamorphism. *J. Petrol.* 44, 1977–2002. <http://dx.doi.org/10.1093/ptrology/egg067>.
- van Hinsbergen, D.J.J., Meulenkamp, J.E., 2006. Neogene supradetachment basin development on Crete (Greece) during exhumation of the South Aegean core complex. *Basin Res.* 18, 103–124.
- van Hinsbergen, D.J.J., Schmid, S.M., 2012. Map view restoration of Aegean–West Anatolian accretion and extension since the Eocene. *Tectonics* 31. <http://dx.doi.org/10.1029/2012tc003132>.
- van Hinsbergen, D.J.J., Hafkenscheid, E., Spakman, W., Meulenkamp, J.E., Wortel, R., 2005. Nappe stacking resulting from subduction of oceanic and continental lithosphere below Greece. *Geology* 33, 325–328. <http://dx.doi.org/10.1130/g20878.1>.
- Waelbroeck, C., Labeyrie, L., Michel, E., Duplessy, J.C., McManus, J., Lambeck, K., Balbon, E., Labracherie, M., 2002. Sea-level and deep water temperature changes derived from benthic foraminifera isotopic records. *Quat. Sci. Rev.* 21, 295–305.
- Wegmann, K.W., 2008. Tectonic geomorphology above Mediterranean subduction zones, northern Apennines of Italy and Crete, Greece. Ph.D. Lehigh University, Bethlehem, PA, p. 169.
- Wells, D.L., Coppersmith, K.J., 1994. New empirical relationships among magnitude, rupture length, rupture width, rupture area, and surface displacement. *Bull. Seismol. Soc. Am.* 84, 974–1002.
- Wijbrans, J.R., McDougall, I., 1986. $^{40}\text{Ar}/^{39}\text{Ar}$ dating of white micas from an Alpine high-pressure metamorphic belt on Naxos (Greece): the resetting of the argon isotopic system. *Contrib. Mineral. Petrol.* 93, 187–194. <http://dx.doi.org/10.1007/BF00371320>.
- Wijbrans, J.R., McDougall, I., 1988. Metamorphic evolution of the Attic Cycladic Metamorphic Belt on Naxos (Cyclades, Greece) utilizing $^{40}\text{Ar}/^{39}\text{Ar}$ age spectrum measurements. *J. Metamorph. Geol.* 6, 571–594. <http://dx.doi.org/10.1111/j.1525-1314.1988.tb00441.x>.
- Willemsse, E.J.M., 1997. Segmented normal faults: correspondence between three-dimensional mechanical models and field data. *J. Geophys. Res.* 102, 675–692. <http://dx.doi.org/10.1029/96jb01651>.
- Willemsse, E.J.M., Pollard, D.D., Aydin, A., 1996. Three-dimensional analyses of slip distributions on normal fault arrays with consequences for fault scaling. *J. Struct. Geol.* 18, 295–309.
- Willett, S.D., Beaumont, C., Fullsack, P., 1993. Mechanical models for the tectonics of doubly vergent compressional orogens. *Geology* 21, 371–374.
- Wortel, M.J.R., Spakman, W., 2000. Subduction and slab detachment in the Mediterranean–Carpathian region. *Science* 290, 1910–1917. <http://dx.doi.org/10.1126/science.290.5498.1910>.
- Zachariasse, W.J., van Hinsbergen, D.J.J., Fortuin, A.R., 2008. Mass wasting and uplift on Crete and Karpathos during the early Pliocene related to initiation of south Aegean left-lateral, strike-slip tectonics. *Geol. Soc. Am. Bull.* 120, 976–993. <http://dx.doi.org/10.1130/b26175.1>.
- Zachariasse, W.J., van Hinsbergen, D.J.J., Fortuin, A.R., 2011. Formation and fragmentation of a late Miocene supradetachment basin in central Crete: implications for exhumation mechanisms of high-pressure rocks in the Aegean forearc. *Basin Res.* 23, 678–701. <http://dx.doi.org/10.1111/j.1365-2117.2011.00507.x>.